

From batch to flow: the effect of pH, current, and crystal facets of Cu₂O on the electrochemical CO₂ reduction

Mathias van der Veer^{a,b}, Nick Daems^a, Pegie Cool^b, and Tom Breugelmans^a

Supporting Information

^a Applied Electrochemistry and Catalysis (ELCAT), University of Antwerp, Campus Drie Eiken, Universiteitsplein 1, 2610 Wilrijk, Belgium

^b Laboratory of Adsorption and Catalysis (LADCA), University of Antwerp, Campus Drie Eiken, Universiteitsplein 1, 2610 Wilrijk, Belgium

Keywords

CO₂ to C₂₊ products, flow electrolyzer, crystal facets, Cu₂O nanocrystals, pH and current effect, electrode stability

Table of content:

Figure S1. In situ Raman flow cell setup

Figure S2. Schematic view of our flow cell setup

Figure S3. SEM of Cu₂O-NF

Figure S4. TEM of Cu₂O-NF

Figure S5. Particle size distribution of Cu₂O-NC

Figure S6. Raman spectrums of Cu₂O-Octahedral, nanoflowers, and nanocubes respectively

Figure S7. XPS images of the different Cu₂O catalysts: (a) Survey profiles, (b) Cu 2p spectra, (c) Cu LM2 spectra, and (d) O 1s spectra.

Figure S8. All of the following CVs were measured ± 50 mV from OCP with scan rates of 25-50-75-100-125 mV s⁻¹. a) Cu₂O-O, b) Cu₂O-NF, c) Cu₂O-NC, d) Cu₂O-O After, e) Cu₂O-NF after, f) Cu₂O-NC After, and g) Linear fit of calculated ECSA, Starting bottom to top, The ECSA of Cu₂O-O (2.44 mF), Cu₂O-NF (4.58 mF), Cu₂O-NC (6.13 mF), Cu₂O-O After (10.69 mF), Cu₂O-NF (17.61 mF), and Cu₂O-NC (22.16 mF)

Figure S9. CO₂RR at 150 mA cm⁻² with Cu₂O-NC for different flow rates at pH 11

Figure S10. CO₂RR at 300 mA cm⁻² with Cu₂O-NC for 1 hour at pH 8.5

Figure S11. Long term stability test of Cu₂O-NF, performed at 150 mA cm⁻² and pH 8.5. The different products are represented at each time interval along with total C₂₊ FE.

Figure S12. Contact angle measurements, off fresh and spent electrolyte on fresh and spent GDE

Figure S13. Contact angle measurements, on a) GDE coated Cu₂O-NC before electrolysis, and b) GDE coated Cu₂O-NC after electrolysis at 150 mA cm⁻². Both were measured after 5 seconds of droplet aging

Figure S14. Long-term stability measurement with single pass 0.5 M KHCO₃ catholyte

Figure S15. SEM measurements for Cu₂O-NC, a) before electrolysis, and b) after electrolysis, with arrows indicating the roughening

Figure S16. XRD spectra taken after electrolysis on GDE compared to the original powder. Spectra given after electrolysis of the different current densities. a) Cu₂O-NC, b) Cu₂O-NF, and Cu₂O-O

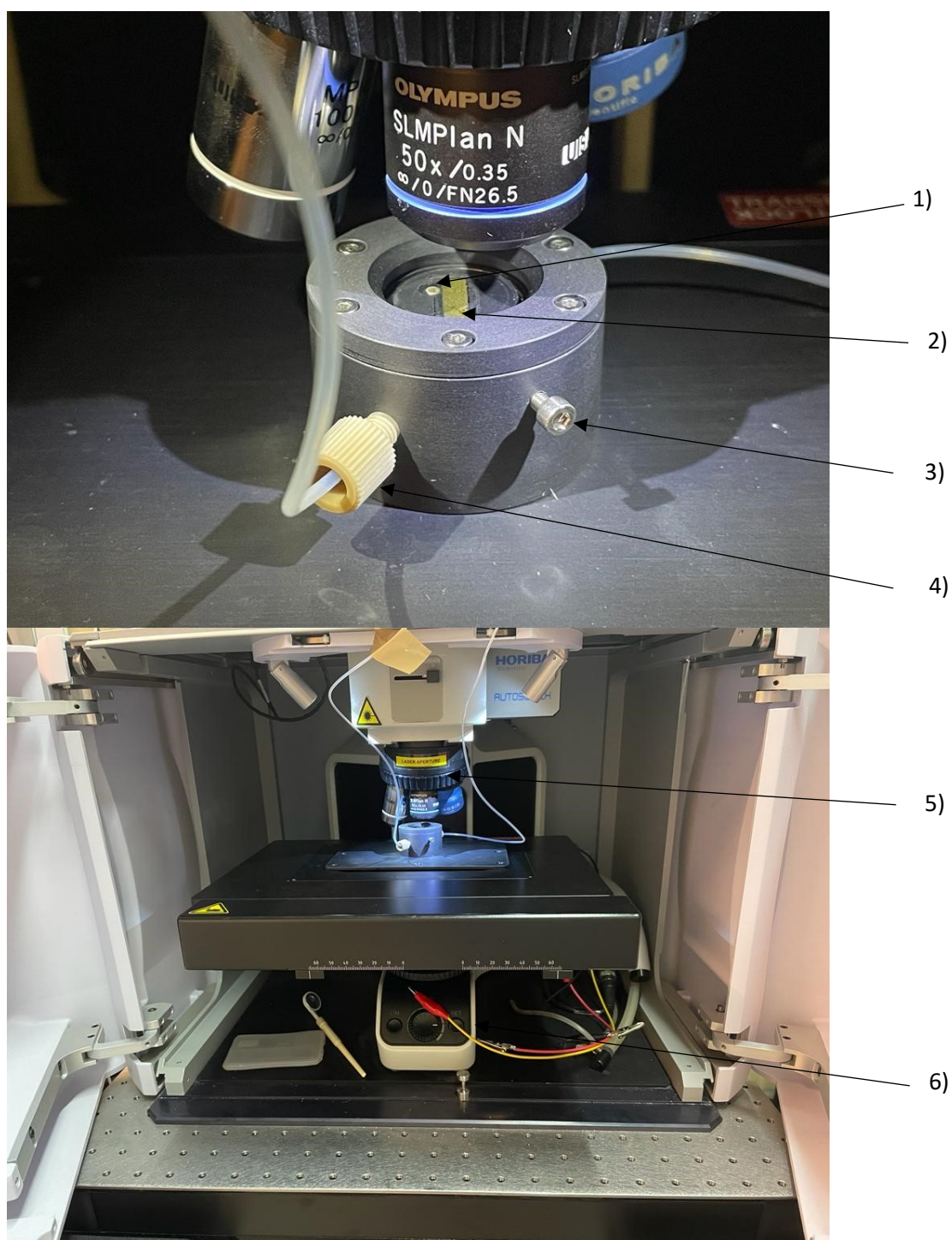


Figure S1. In situ Raman flow setup. 1) reference electrode Ag/AgCl, 2) GDE as working electrode with gold finger, 3) connection to working electrode, 4) flow channels for electrolyte, 5) Raman laser, and 6) electrical connections to reference- and counter electrode.

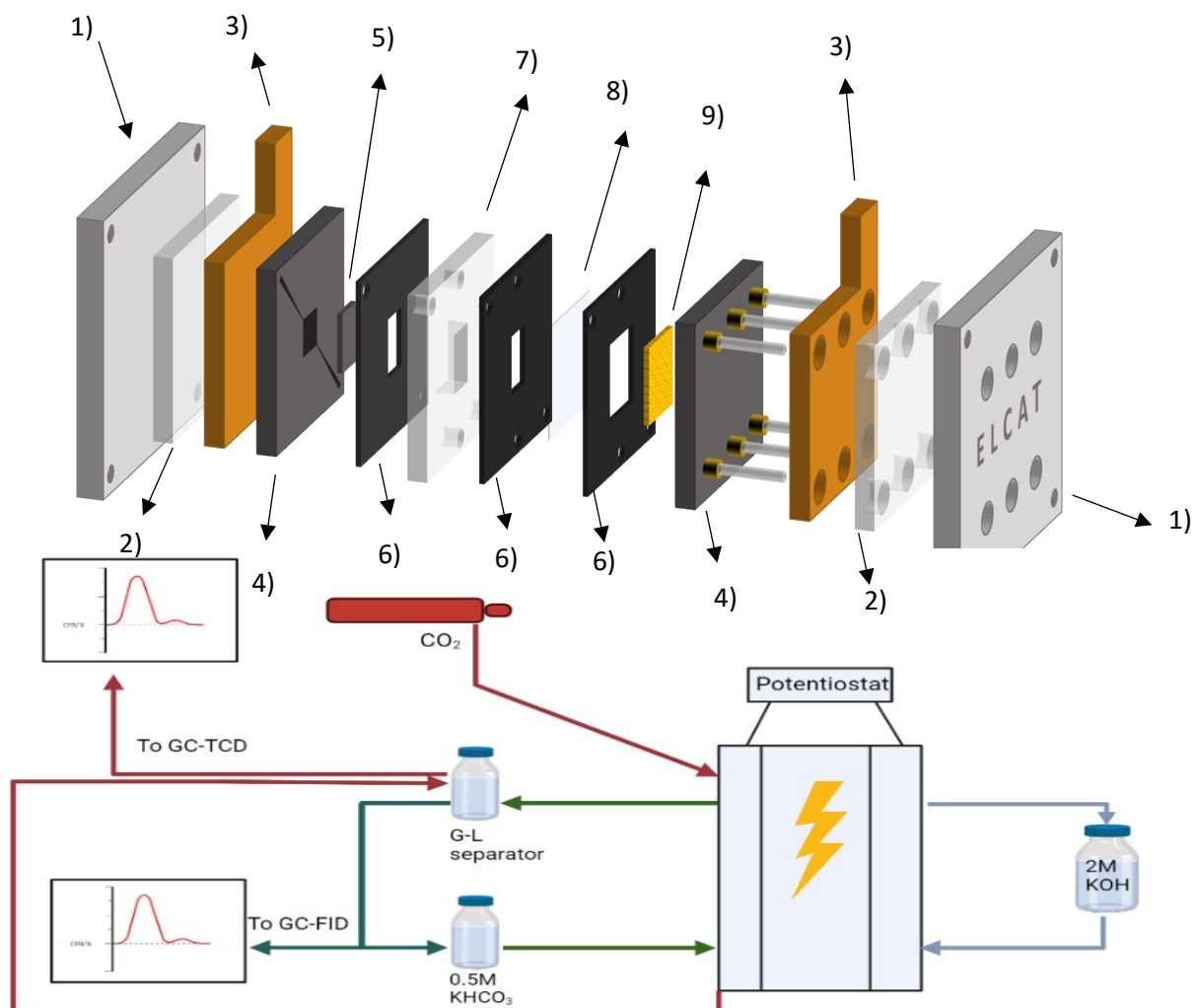


Figure S2. A schematic view of the electrochemical CO₂ reduction, along with an in depth depiction of the flow cell. 1) Aluminum plates, 2) PMMA isolation plates, 3) Conductive copper plates, 4) Flat designed graphite substrate plates without vortex generators, 5) Catalyst coated GDE, 6) Rubber gaskets, 7) Reference electrode holder, 8) Nafion 117 membrane, and 9) Nickel foam anode

Liquid samples for the detection of alcohols were prepared as follows: 1 mL of sample was added to a vial with 100 μ L 1% Butanol as Internal standard (IS), which was uniformly mixed. Another vial was prepared which contained 100 μ L of IS, 1% ethanol, and 1% 1-propanol, diluted with water to a total volume of 1.1 mL. The areas of the standard mixture were used to calculate the amount of ppm of product present in the sample, the internal standard was used for the correction. Based on the ppm, the faradaic efficiency was calculated. For the detection of formic acid, 1 mL of sample was combined with 1 mL of 1.2 M of HClO₄ to precipitate the salts. Then, 1 mL of this mixture was analyzed with HPLC (Diluted x2) and compared with a standard of 100 ppm formic acid.

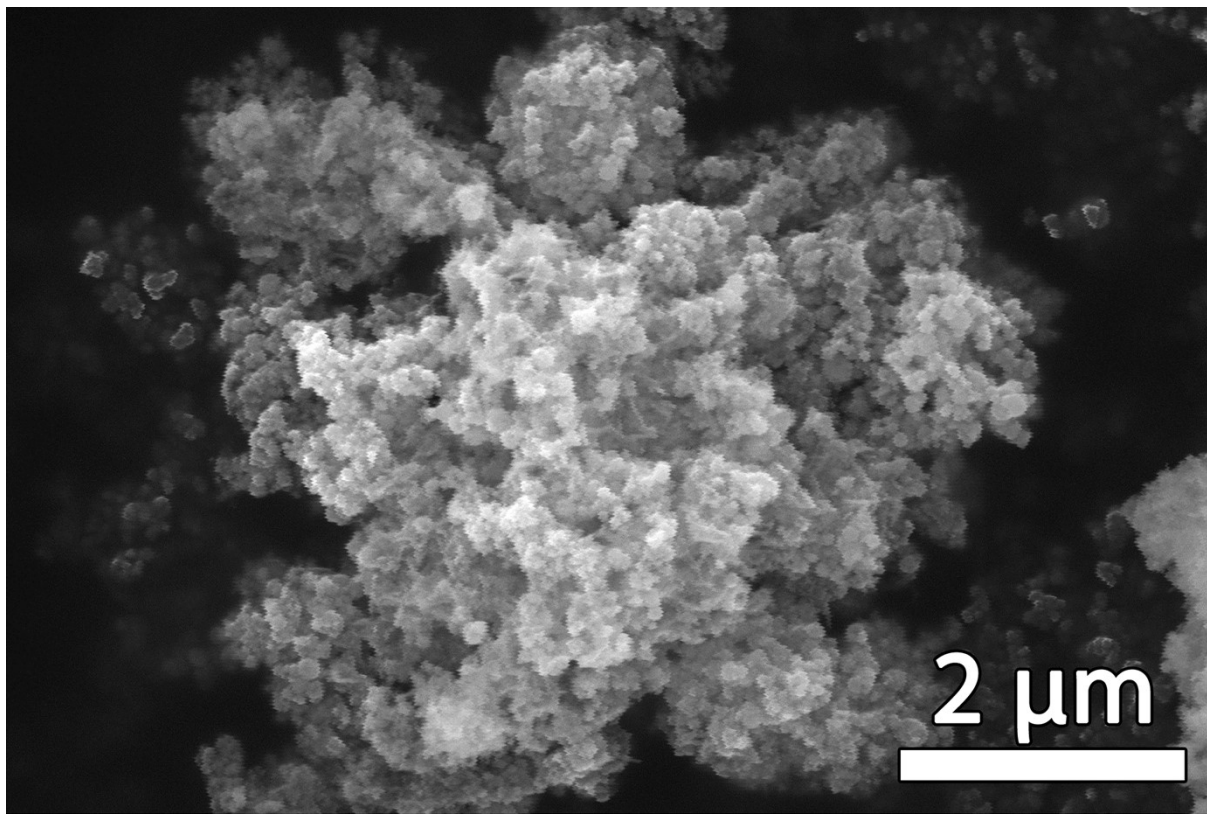
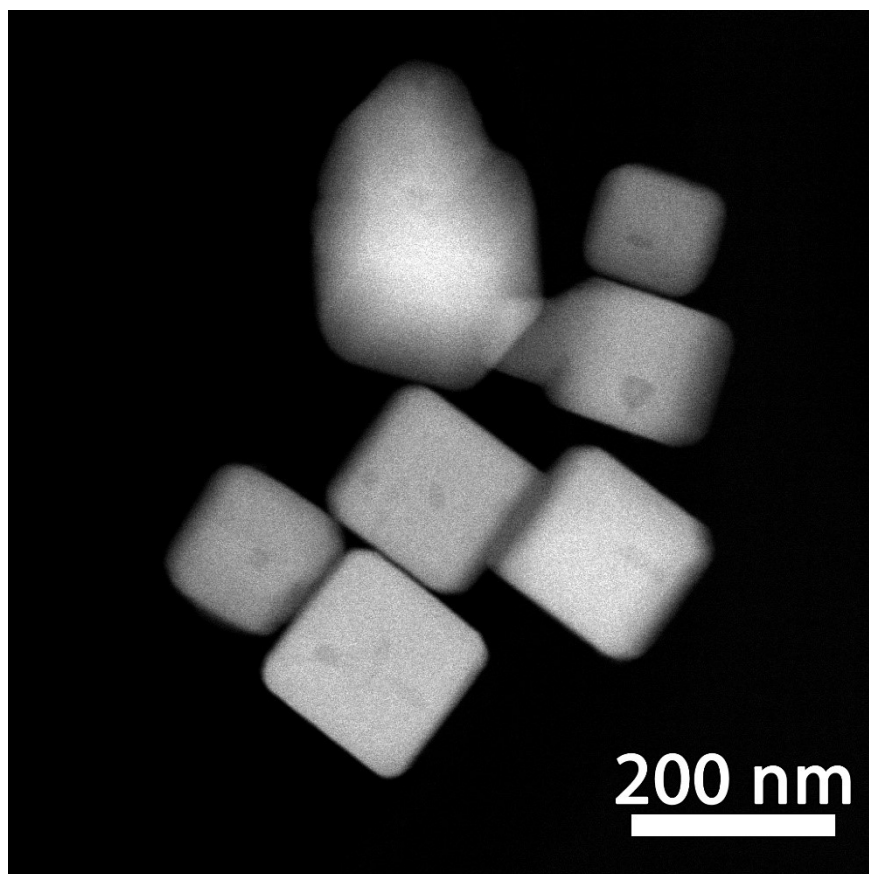


Figure S3. SEM image of Cu₂O-NF

a)



b)

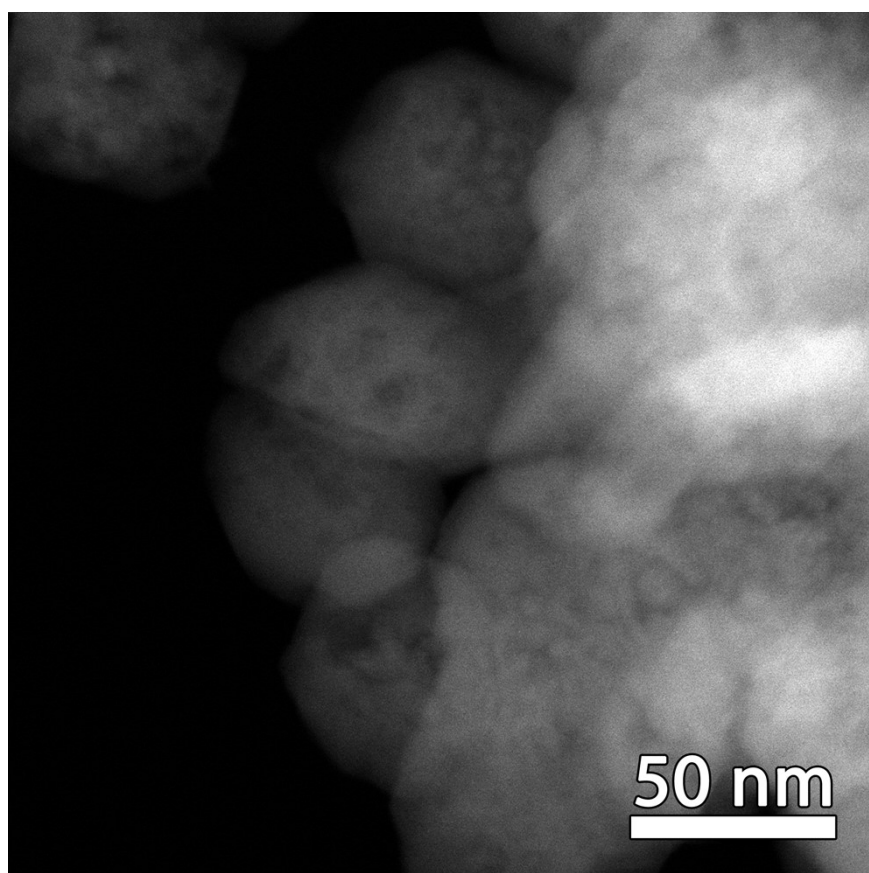


Figure S4. TEM images of a) Cu₂O-NC, and b) Cu₂O-NF

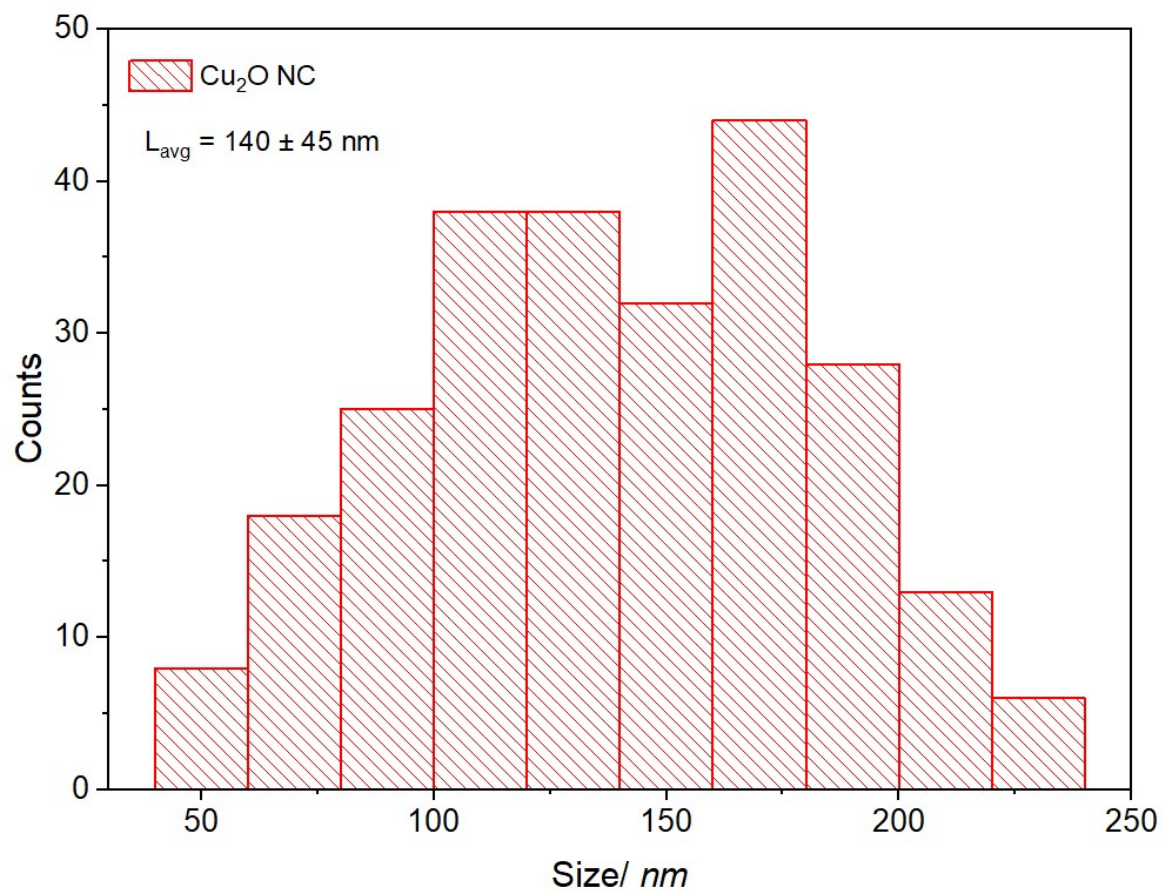


Figure S5. Particle size distribution histogram of Cu₂O-NC, 300 particles were used for the calculations, with the edge length as the value that was used for calculating the size.

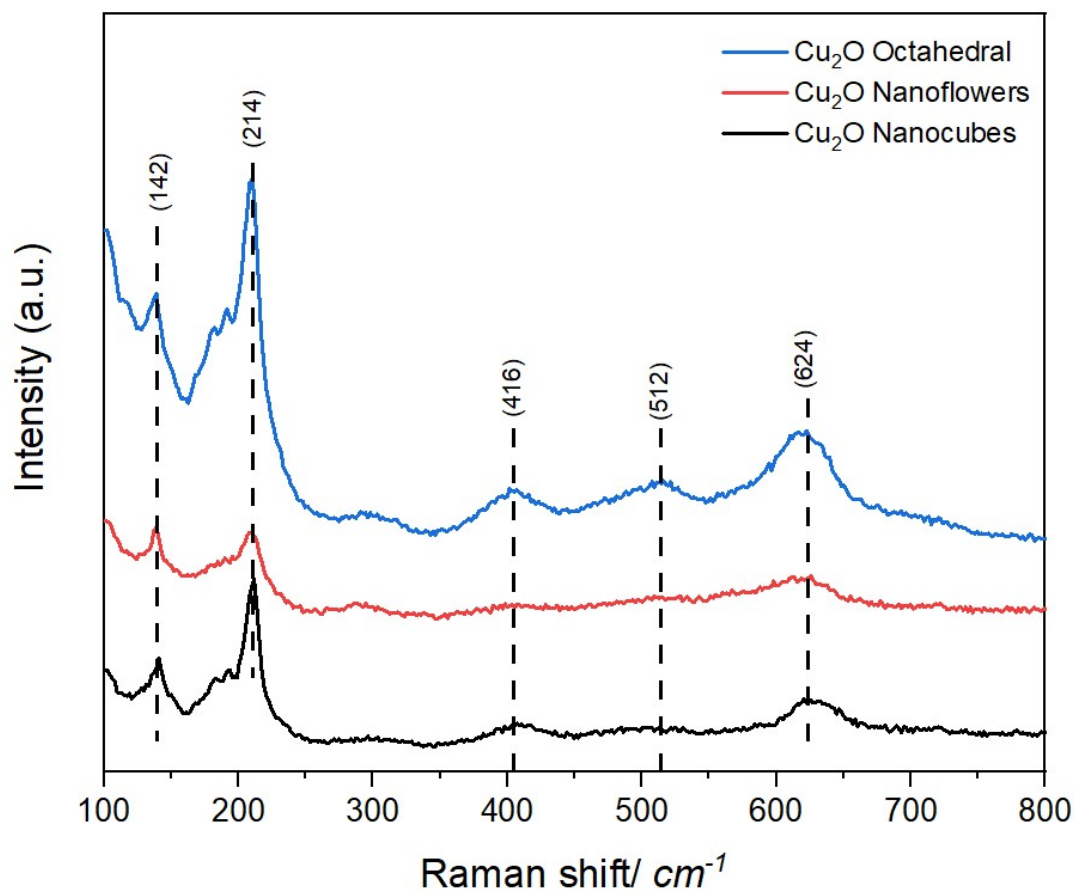


Figure S6. Raman spectrums of Cu₂O-Octahedral, nanoflowers, and nanocubes respectively

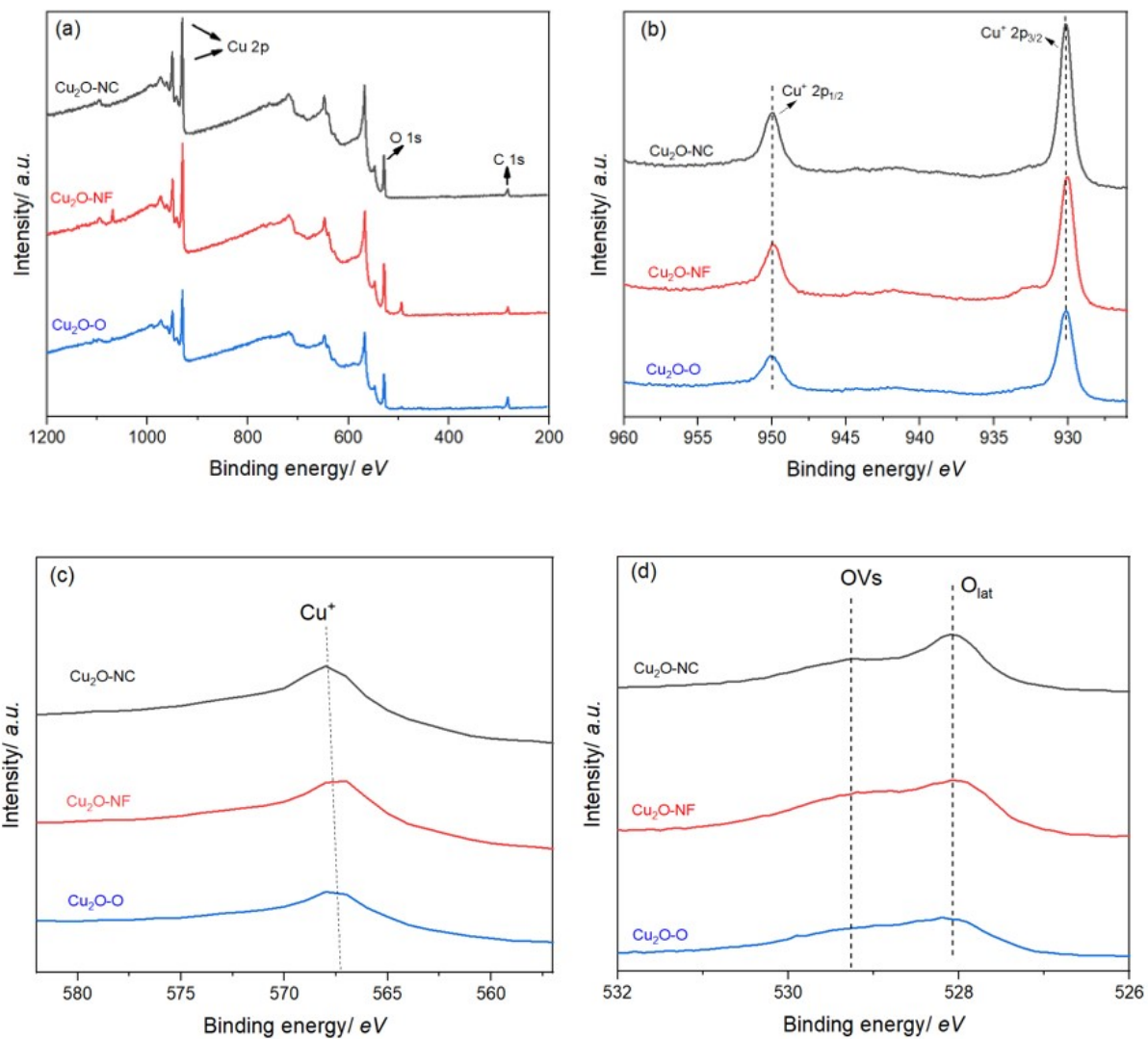
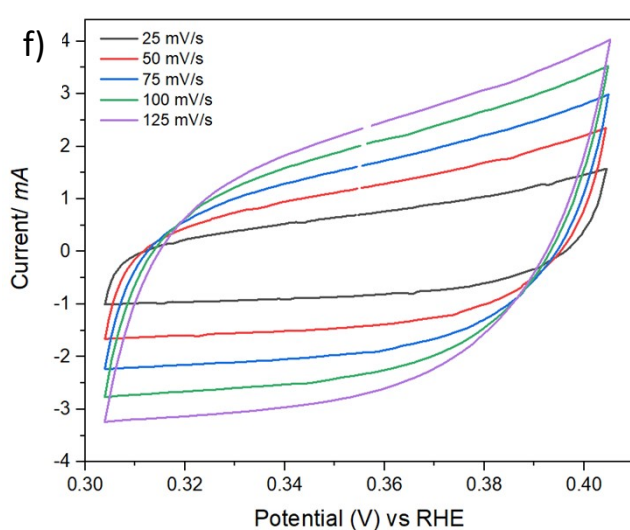
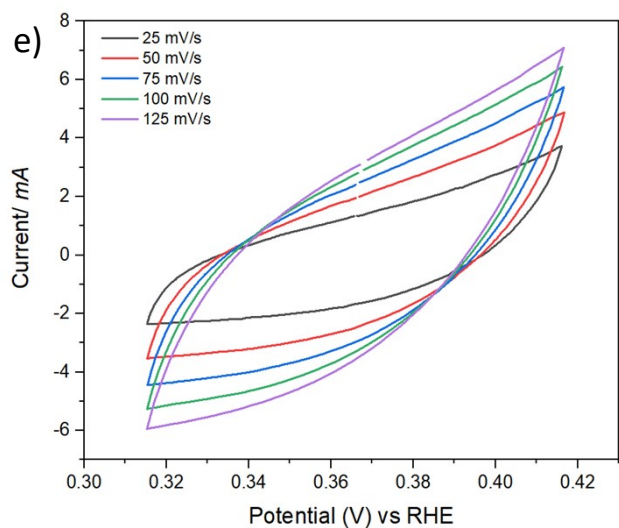
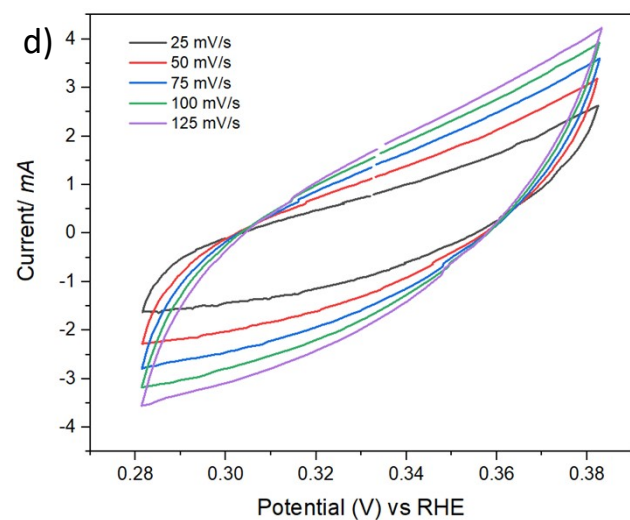
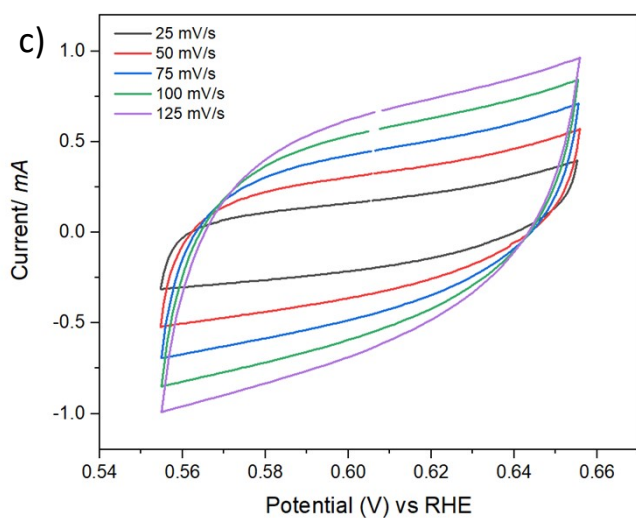
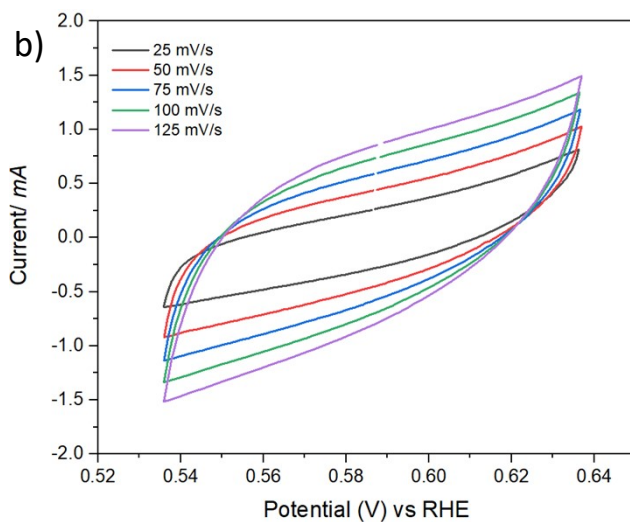
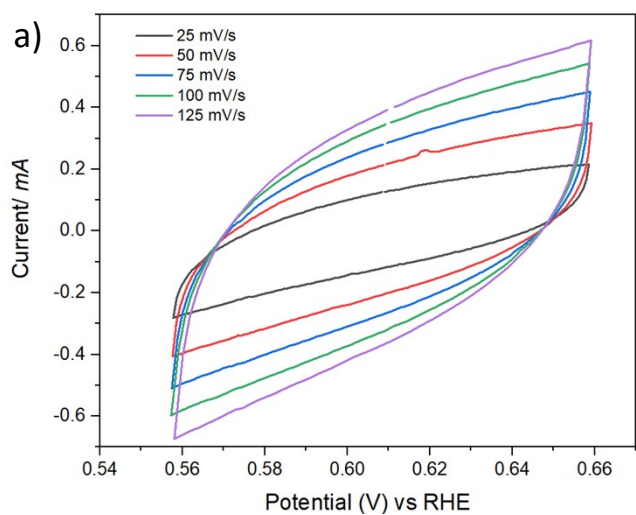


Figure S7. XPS images of the different Cu₂O catalysts: (a) Survey profiles, (b) Cu 2p spectra, (c) Cu LM2 spectra, and (d) O 1s spectra.



g)

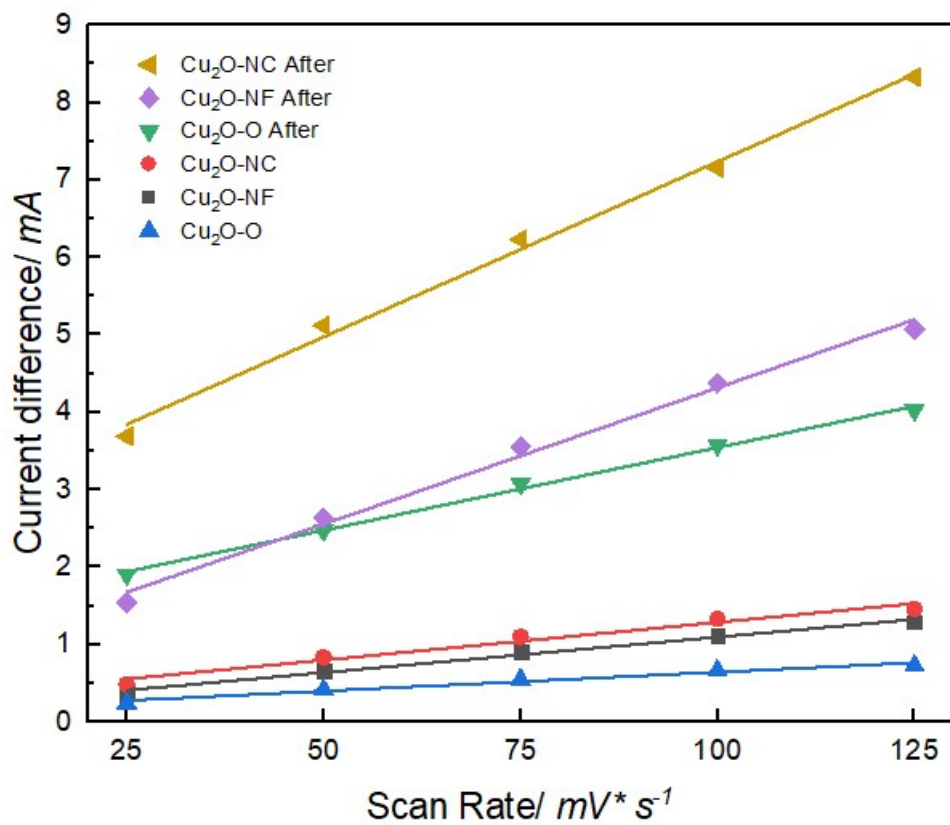


Figure S8. All of the following CVs were measured ± 50 mV from OCP with scan rates of 25-50-75-100-125 $mV s^{-1}$. a) Cu₂O-O, b) Cu₂O-NF, c) Cu₂O-NC, d) Cu₂O-O After, e) Cu₂O-NF after, f) Cu₂O-NC After, and g) Linear fit of calculated ECSA, Starting bottom to top, The ECSA of Cu₂O-O (5.21 mF), Cu₂O-NF (9.7 mF), Cu₂O-NC (11.29 mF), Cu₂O-O After (21.38 mF), Cu₂O-NF (35.23 mF), and Cu₂O-NC (45.25 mF)

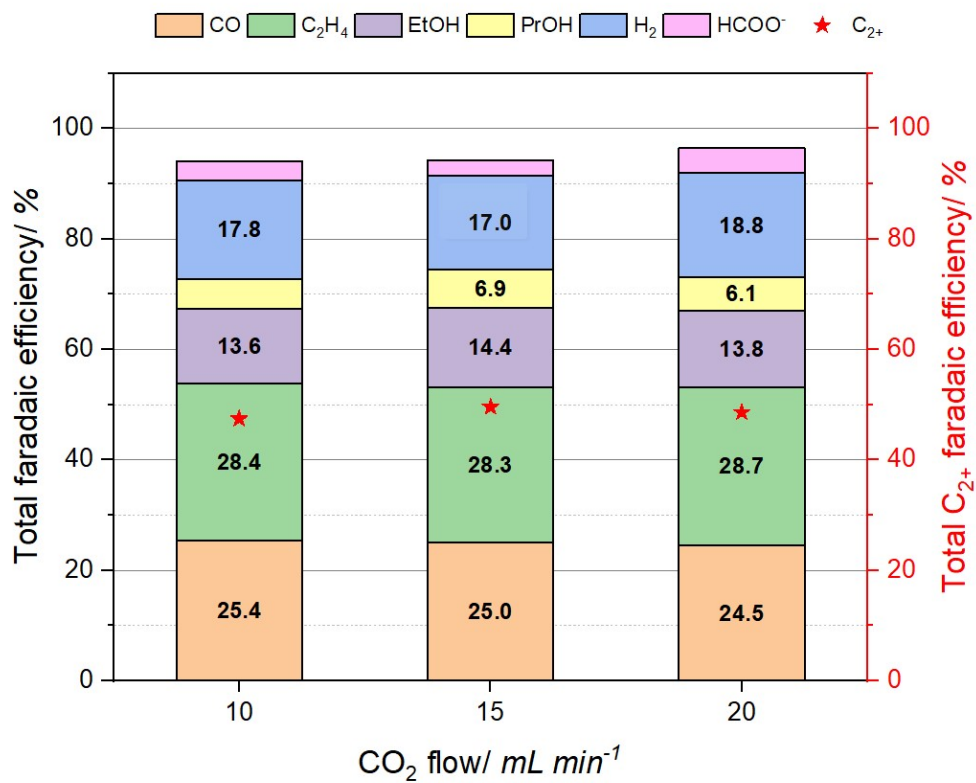


Figure S9. CO₂RR at 150 mA cm⁻² with Cu₂O-NC for different flow rates at pH 11

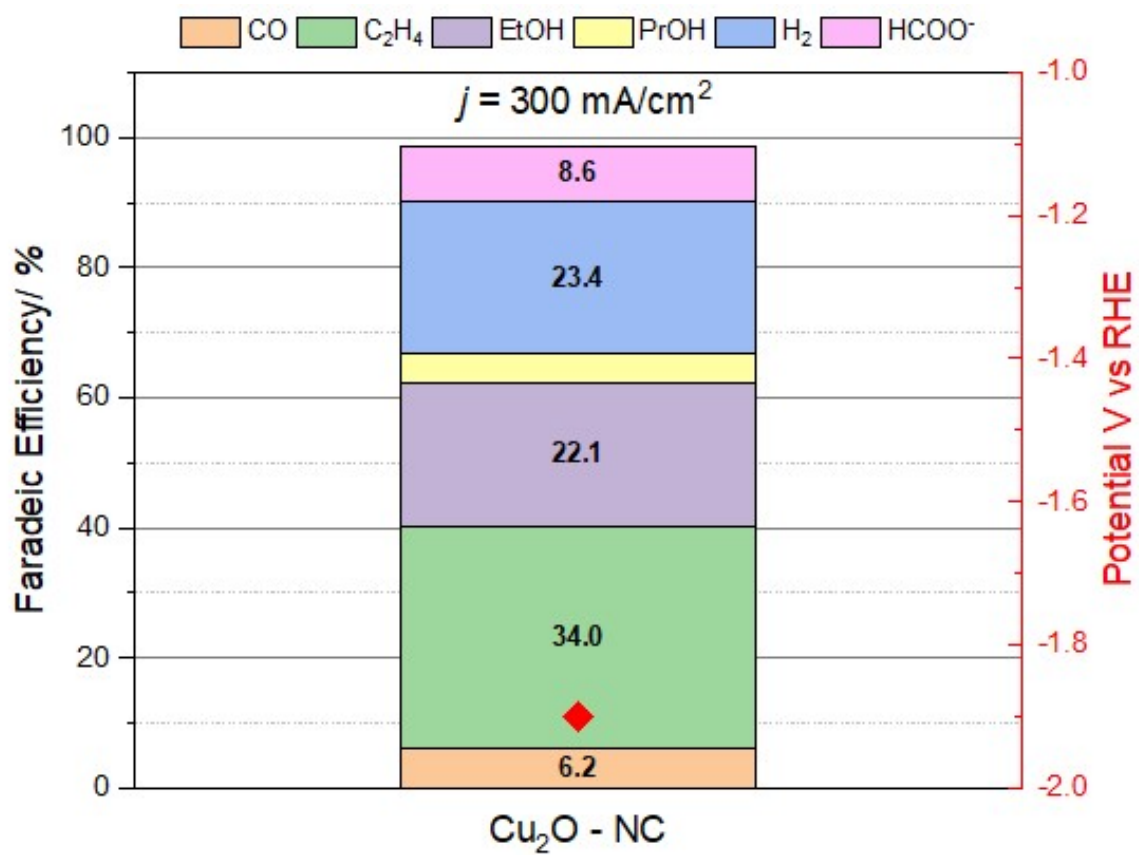


Figure S10. CO₂RR at 300 mA cm⁻² with Cu₂O-NC for 1 hour at pH 8.5

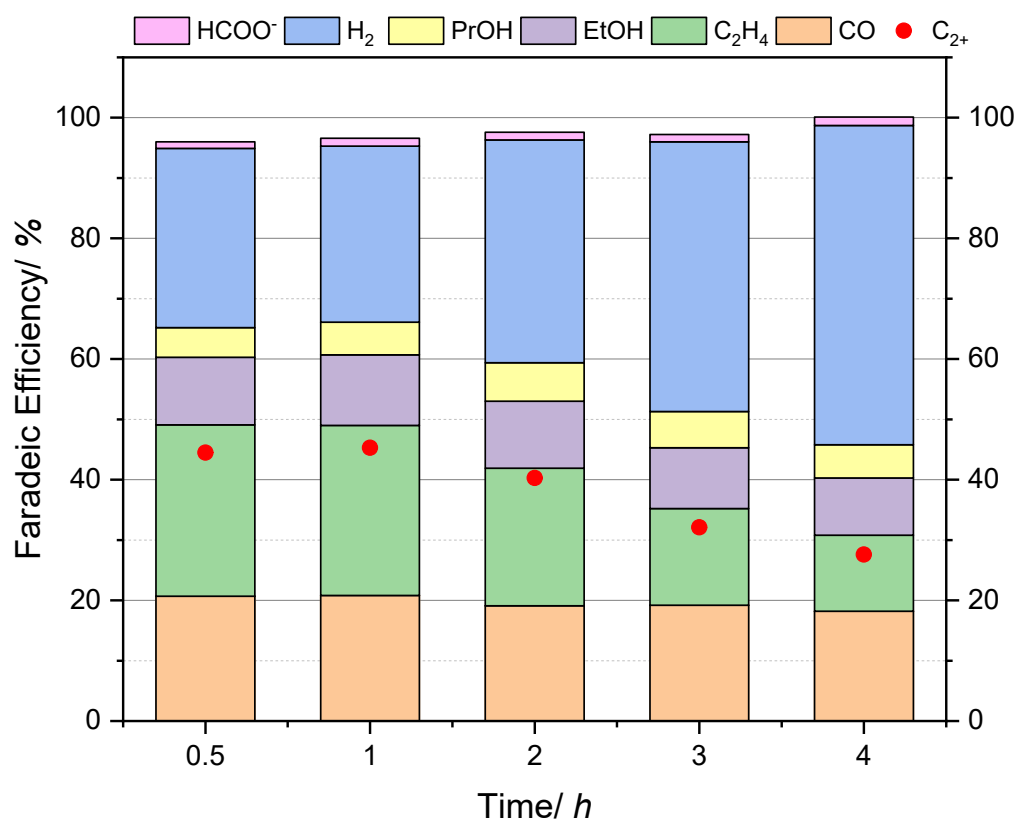


Figure S11. Long term stability test of Cu₂O-NF, performed at 150 mA cm⁻² and pH 8.5. The different products are represented at each time interval along with total C₂₊ FE.

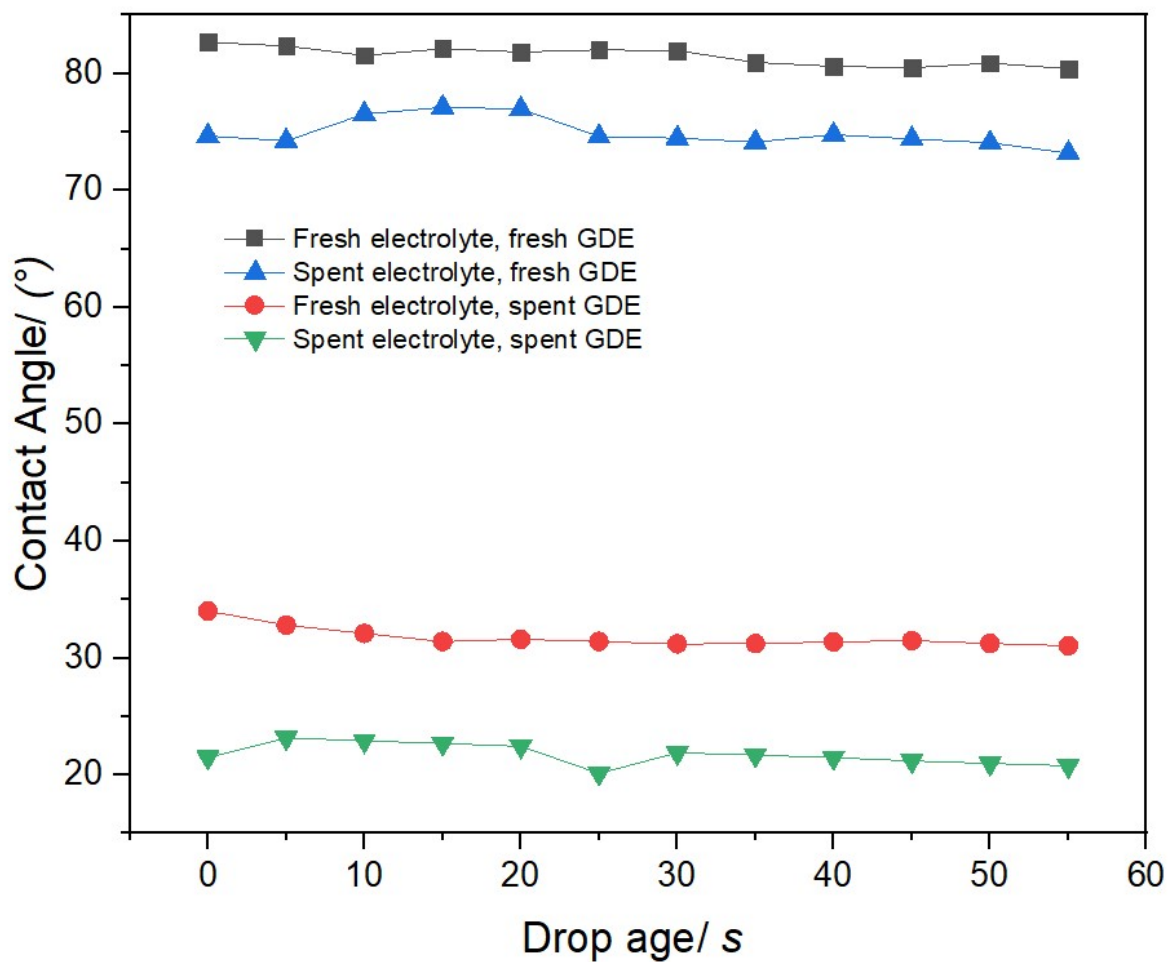
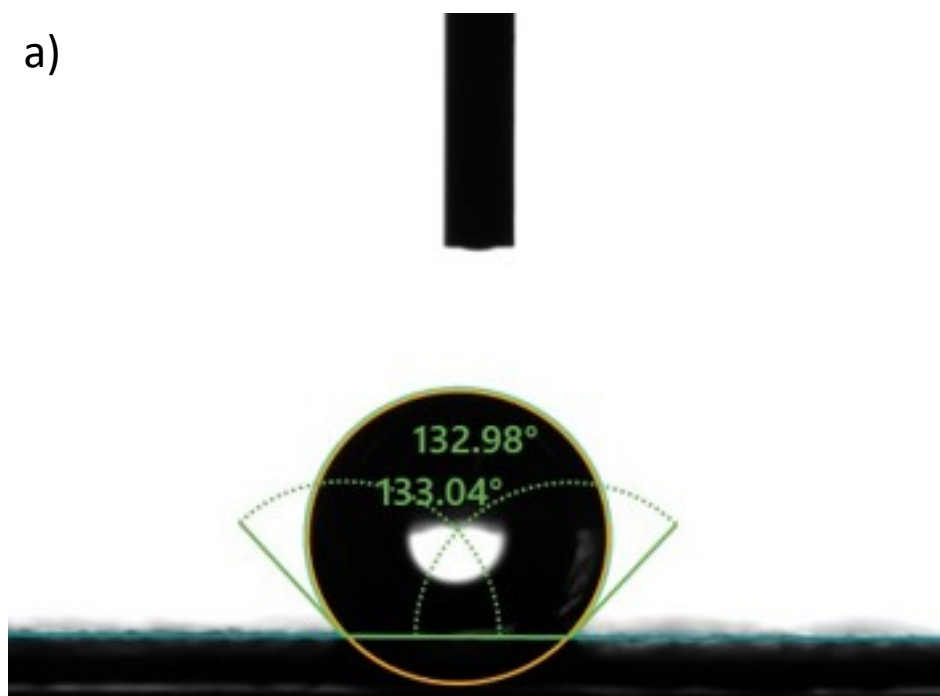


Figure S12. Contact angle measurements, off fresh and spent electrolyte on fresh and spent GDE

a)



b)

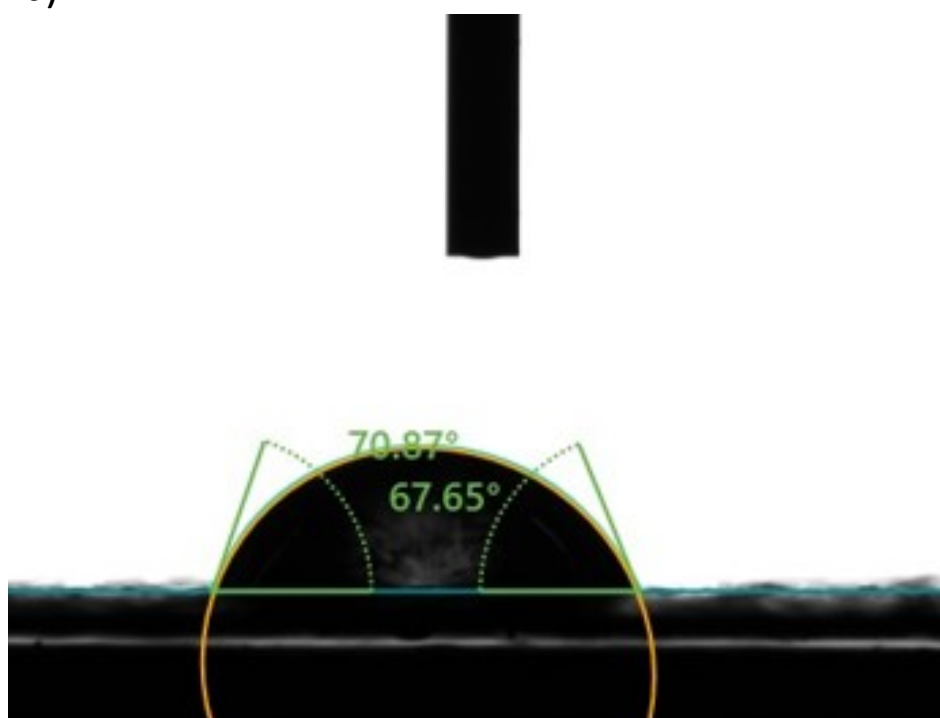


Figure S13. Contact angle measurements, on a) GDE coated $\text{Cu}_2\text{O-NC}$ before electrolysis, and b) GDE coated $\text{Cu}_2\text{O-NC}$ after electrolysis at 150 mA cm^{-2} . Both were measured after 5 seconds of droplet aging

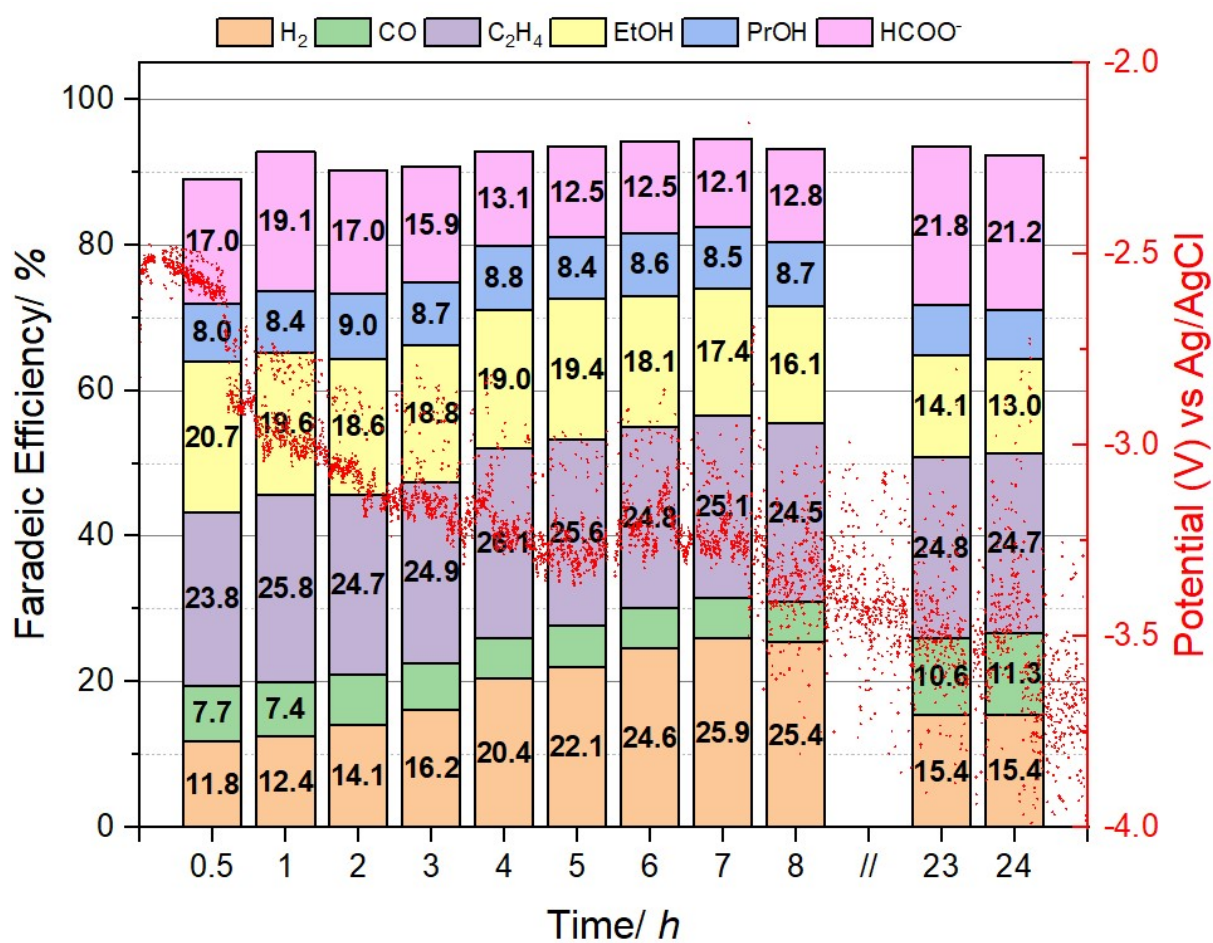


Figure S14. Long-term stability measurement with single pass 0.5 M KHCO₃ catholyte

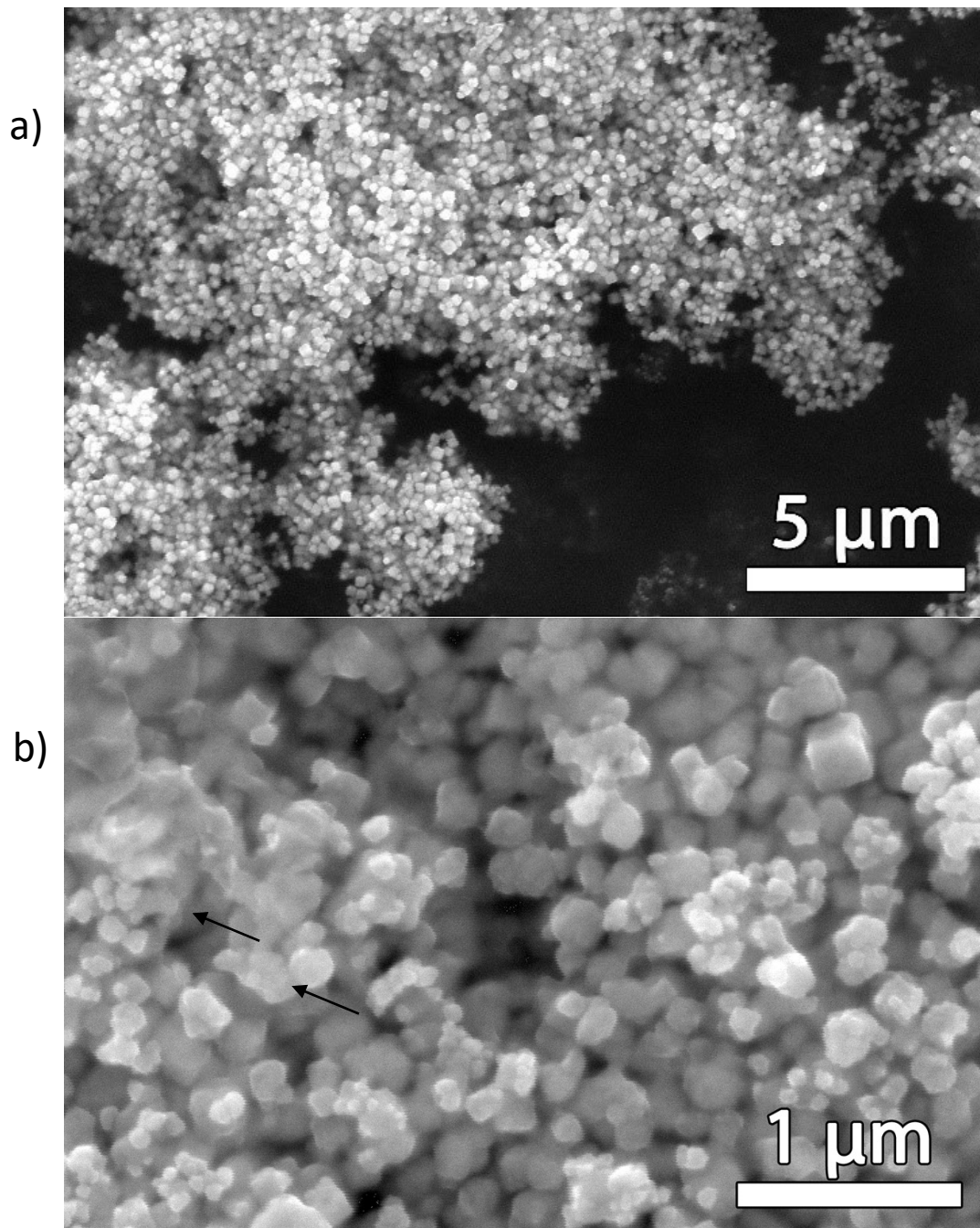


Figure S15. SEM measurements for Cu₂O-NC, a) before electrolysis, and b) after electrolysis, with arrows indicating the roughening

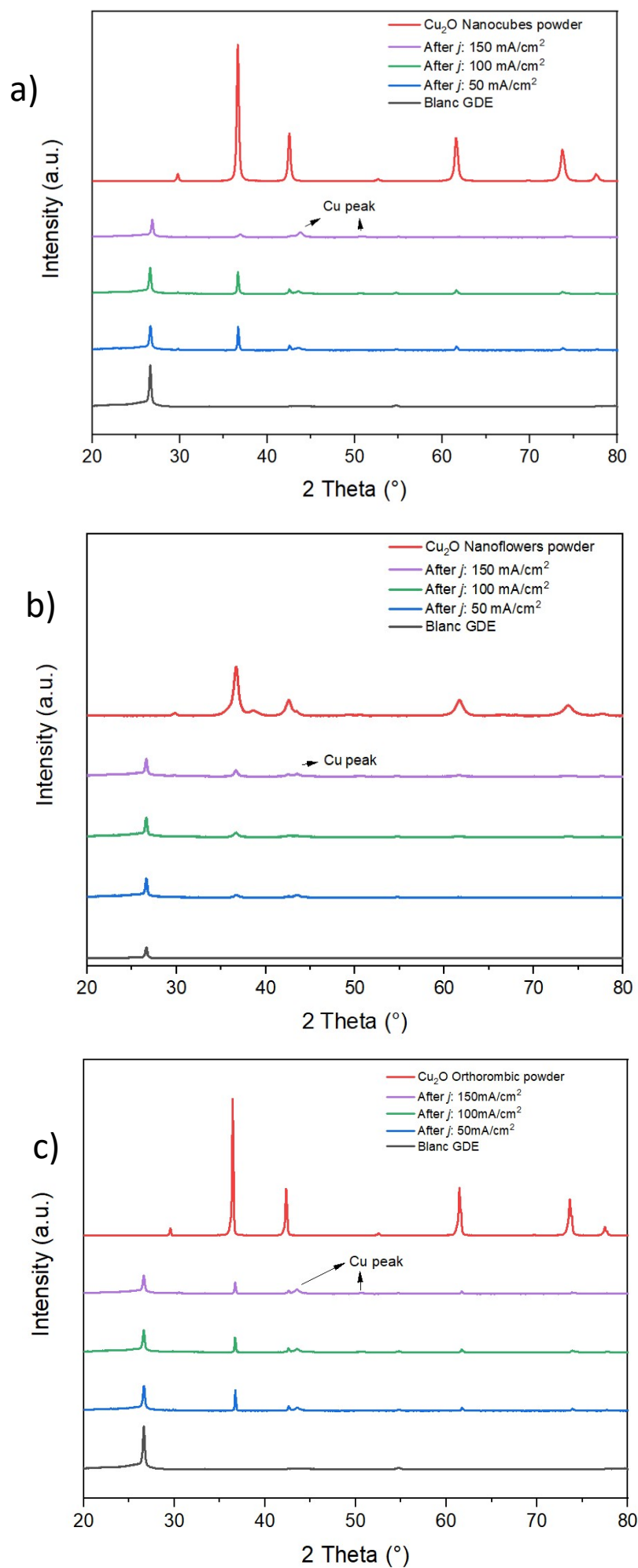


Figure S16. XRD spectra taken after electrolysis on GDE compared to the original powder. Spectra given after electrolysis of the different current densities. a) Cu_2O -NC, b) Cu_2O -NF, and Cu_2O -O